Please do not delete comment balloons and do not accept all changes.

In situ **scanning electrochemical probe microscopy for energy applications**

Stanley C.S. Lai, Julie V. Macpherson, and Patrick R. Unwin

High resolution electrochemical imaging methods provide opportunities to study localized phenomena on electrode surfaces. Here, we review recent advances in scanning electrochemical microscopy (SECM) to study materials involved in (electrocatalytic) energy-related applications. In particular, we discuss SECM as a powerful screening technique and also advances in novel techniques based on micro- and nanopipets, such as the scanning micropipet contact method and scanning electrochemical cell microscopy and their use in energy-related research.

Keywords: Scanning probe microscopy (SPM), energy generation, surface chemistry, catalytic

Introduction

The increased concern about the future availability of fossil fuels as the main energy source has spurred a renewed interest in the search for alternative energy sources and technologies.[1] Examples of such new technologies include (low temperature) fuel cells and new types of batteries and solar cells, which convert chemical or radiant energy into electrical energy for consumption. These technologies, and the associated challenges, are centered on electrochemistry, and electrochemical tools are needed to study these systems.

The main challenge in studying many of these new energy systems lies in the complex electrode-electrolyte interface. In particular, the efficiency of such systems is determined by the interplay between the nature (material and structure) of the electrode, mass transport of reactants and products to and from the electrode, and the surface reactivity, all of which are strongly localized on the

nanoscale. Traditionally, most electrochemical techniques have been limited to the investigation of the entire electrode-electrolyte interface, such that only average properties can be elucidated. A truly fundamental understanding of these systems can only be gained from localized studies, ultimately with the capability of probing at the nanoscale.

The aim of this contribution is to give an overview of the application of *in situ* scanning electrochemical probe microscopy (SEPM) techniques used in energy-related studies. This is a broad and rapidly expanding area, and so the particular focus is on the use of novel SEPM techniques for obtaining fundamental information at the micro- and nanoscale to investigate truly localized processes.

Scanning electrochemical microscopy

Since its introduction in the late 1980s, scanning electrochemical microscopy (SECM)[2,3] has developed into a powerful technique to probe electrochemical processes, primarily on the microscale for a wide variety of applications.[4–7] In brief, SECM employs an ultramicroelectrode (UME), often called "tip" in analogy with other scanning probe techniques, positioned near the substrate of interest. An UME consists of a micro- or nanoscale electrode sheathed in an insulating material to minimize back diffusion, thus making the tip more sensitive to the process occurring at the substrate. A typical SECM setup is described in detail in Reference 2. The electrochemical (typically current) response of the tip is used to provide information on local properties such as topography and/or reactivity. Various modes of operation can be employed (**Figure 1**a–d).[4,5] For the study of electrode surfaces, the UME is typically used to (1) electrochemically detect (collect) the product generated at the electrode (substrate generation/tip collection; SG/TC); (2) generate a reactant for reaction at the substrate (tip generation/substrate collection; TG/SC); or (3) generate a reactant at the tip that can be converted at the substrate and regenerated at the tip (feedback mode). The tip and substrate can also be set to compete for a redox-active species in a classical shielding[8] or equivalent redox competition mode.[9]

The tip can either be held in a fixed position or scanned over the *xy*-plane, with the currents at the tip and substrate recorded as a function of tip position, providing a two-dimensional image of (local) reaction rates from which quantitative information can be extracted. The spatial resolution in SECM depends strongly on the electrode diameter (generally 5–50 μm) and the tip-to-substrate separation. In conventional SECM, the tip is scanned at constant height (fixed *xy*-plane), as there is no feedback mechanism to maintain a constant tip-to-substrate separation. Consequently, this requires the sample to be flat and well-aligned, and the tip-to-substrate separation to be set sufficiently large (generally one electrode radius) to prevent tip crash.

Advances in SECM have been reviewed extensively,[4–7,10,11] including a recent comprehensive treatment of the use of SECM in energy-related applications by Bertoncello.[11] Here, we provide a brief summary of the use of SECM as a screening technique in energy research, as this is a particularly powerful application of the method (Figure 1e).

SECM has been employed extensively as a tool for electrocatalyst screening for the hydrogen oxidation and evolution reactions (HOR/HER) and the oxygen reduction and evolution reactions (ORR/OER), which are of potential interest for use in (low temperature) fuel cells. The approach taken generally is to prepare arrays of electrocatalysts of different compositions on a conductive material with poor electrocatalytic activity (such as indium tin oxide (ITO) or carbon materials). Such arrays can be imaged rapidly for electrocatalytic activity and the most promising samples identified for further detailed examination. Figure 1e shows a typical example of an SECM image of such an array, in this case highlighting variations in the activity of binary Pd-Co alloys of varying composition (supported on glassy carbon) towards the ORR in 0.5 M H_2SO_4

Initially, catalyst screening studies were conducted in feedback mode for the HOR, as the H^+/H_2 redox couple is facile and can be followed accurately using a platinum tip. While the most efficient catalyst for the HOR is platinum, it is easily deactivated by CO, a common feedstock contaminant in H_2 fuel cells. There is ongoing research into minimizing this deactivation. A common strategy

is to modify the Pt catalyst with a second (and third) material that catalyzes the oxidative removal of CO while maintaining the activity of Pt. The extensive number of potential materials and compositions necessitates the need for quick catalyst screening methods, such as SECM. Interesting early SECM screening for HOR catalysts was performed by Hillier et al. who studied the HOR on Pt_xRu_y[12,13] and $Pt_xRu_yMo_z$,[12] in the absence and presence of CO. Introducing small amounts of Ru (20-30%) and Mo (10-25%) to Pt was found to significantly increase the CO tolerance, leading to the lowest onset potential for the HOR in the presence of CO. Similarly, McGinn et al. employed SECM for the rapid screening of Pt-Ru,[14] Pt-Ru-WC[15] and Pt-Ru-Co[15] thin film libraries, containing arrays of hundreds of different compositions on a single sample, and found similar synergistic effects of Ru and WC or Co towards the catalyst's CO tolerance. Such findings demonstrate the power of SECM to quickly assess the reactivity for a large number of material compositions, which is expected to aid in the rational design of catalysts for H_2-fuel cell development.

While the feedback mode is well suited for studying the HOR, it cannot be employed to study the ORR, as the generated product is water. Bard et al. thus introduced the tip generation/substrate collection (TG/SC) mode to screen Pt-free electrocatalysts (various combinations of Pd, Au, and Ag with Co,[16–18] Ti,[17] V,[19] and/or Mn[19]) for the ORR. It was found that while not all combinations showed synergistic effects, several came close in performance to a conventional Pt electrode.[18,19] Similarly, Herrero et al. studied the ORR at shape-controlled gold nanoparticles (NPs) and found that cubic NPs, which have a high abundance of (100) facets, were the most active, consistent with results obtained on macroscopic Au(100).[20,21]

SECM has also been employed by Bard's group to study photocatalysts[22,23] for the conversion of solar energy to electricity or fuels and to screen porphyrins for use as Ru-free sensitizers for dye-sensitized solar cells (or Grätzel cells).[24] A gold coated optical fiber was used as the tip, with the optical core used to photoactivate the catalyst. The photocatalytic response was measured as the substrate current on a spot by spot basis. The gold ring electrode on the tip

could be further functionalized to electrochemically detect the product of the substrate reaction.[22,23] Using this configuration, the activity of various $BiVO_4$ based photocatalysts was screened.[23] The most active catalyst for water oxidation was found to be $BiVO_4$ with a 5-10% addition of W, and the production of oxygen (the product of water oxidation) was further quantified at a Pt functionalized Au ring electrode. [23] Finally, conventional SECM approach curve measurements have proven powerful in detailed studies of photocatalysts and photovoltaic materials and have yielded insight in the correlation between optical and electrochemical properties of semiconductors[25] and in the kinetics of various processes in dye-sensitized solar cells.[26,27]

Although (conventional) SECM is well suited to screen the reactivity of different materials, its spatial resolution is generally limited to the µm-range or greater, and nanoscale reactivity studies are rare or non-existent. Efforts to increase the spatial resolution involve moving toward nanometer-sized tips,[28–30] and reliably decreasing the tip-to-substrate separation.[31] Such moves generally require the incorporation of positional feedback into SECM, allowing the tip to follow the substrate at a small and constant separation.[32–44]

Combined -SECM- AFM (atomic force microscopy)[33–36] is one of the most documented hybrid SECM modes. By integrating a micro/nanoelectrode in an AFM probe, the surface topography can be tracked accurately with AFM, while the electrochemical properties of a substrate can be measured using SECM. The key aspect in SECM-AFM development is the design and preparation of combined (integrated) SECM-AFM probes (see Reference 32 and references therein). SECM-AFM probes can be, typically, divided into two broad categories. Firstly where the electrode for SECM measurements is located at the apex of the AFM tip and secondly where the electrode is placed a set distance away from the tip apex. Examples of both designs are shown in Figure 2. Thus far, combined SECM-AFM studies on energy-related systems are mostly limited to studies on the intrinsic electron transfer properties of support materials for electrocatalytic NPs.[45-46] Frederix et al.[45] and Demaille et al.,[46] for example, have employed SECM-AFM to study various conductive substrates and demonstrated that highly

oriented pyrolytic graphite (HOPG)[45,46] and MoS_2,[45] two model catalyst support materials, exhibit electron transfer activity comparable to gold and platinum, at least initially. Such findings are important in understanding the role of the catalyst support in the overall catalytic activity.

Alternatively, attempts have been made to incorporate SECM functionality into an electrochemical scanning tunneling microscopy (EC-STM) setup, as the requirements for the tip are similar.[37-41] An elegant study using SECM-STM by Stimming et al.[39] (Figure 3) involved electrodepositing a single Pd NP on the tip and subsequently transferring it to a gold substrate. After transfer, the SECM-STM tip, located ~10 nm from the NP, was used to investigate the HER in SG/TC mode by detecting H_2. Afterward, the size of the NP was fully characterized using the STM functionality of the combined probe. It was found that small Pd NPs (0.5 nm high, 6 nm diameter) were two orders of magnitude more active than larger particles (10 nm high, 200 nm diameter).[39] As there is a drive towards smaller NPs to optimize metal utilization, this methodology can be used to determine the optimal NP size.

Pipet-based scanning probe methods

Although SECM is a powerful technique for investigating local substrate reactivity, it has three main shortcomings. First, the lateral resolution can be limited due to coupling between active sites on the substrate and the tip, such that the exact region of the substrate probed is not clearly delineated. Furthermore, SECM requires the entire sample to be submerged in the electrolyte solution during an experiment, which could potentially lead to a change in surface properties due to adsorption or corrosion processes. Finally, SECM has generally required the use of electrochemically active specieswhich readily undergo redox reactions at the tip and substrate electrodes, making it less suited for more complex electrochemical reactions.

Pipet-based imaging methods overcome many of these problems and can be traced back at least as far as capillary based droplet cells, used mainly for corrosion studies.[47-49] The scanning micropipet contact method (SMCM, **Figure 4**a–b) advances these methods by employing small pipets as the probe (typically

between 10 μm and 1 mm diameter, although capillaries as small as ~500 nm have been reported) filled with an electrolyte solution.[48] The liquid meniscus of electrolyte solution protruding from the end of the pipet is brought into gentle contact with the substrate, where it is held by surface tension[47,48] or, for the case of most droplet cells, by a silicon rubber gasket between the mouth of the capillary and the substrate.[47,49] The filled capillary is connected to counter/reference electrodes, while the wetted area of the substrate defines the working electrode, thereby forming a conventional two- or three-electrode dynamic electrochemical cell, and, consequently, all conventional electrochemical techniques can be used. As the area under investigation is limited by the contact area of the droplet, SMCM and droplet cells generally are especially useful to make individual measurements on specific surface locations.

SMCM has been employed to address various energy-related issues. For example, SMCM was used to investigate the kinetics of Pd,[50] Pt,[50] and Au[51] NP electrodeposition on pristine carbon nanotube (CNT) networks. CNT networks are employed in numerous electrical applications. However, most applications as well as fundamental research require a well-defined exposed area of the CNT network. This is normally achieved by time consuming lithographic processing, which can also lead to surface contamination. SMCM circumvents the need for lithographic processing and allows many electrodeposition measurements on the same sample, systematically varying parameters by simply moving the position of the microcapillary By varying deposition potential and time, followed by AFM and scanning electron microscopy (SEM) analysis of the formed particles, the parameters influencing the density, distribution, and size of NPs have been identified. Schuhmann et al. utilized SMCM to deposit clusters of Pt, Au, Rh, and Ru (and combinations thereof) NPs on a CNT network, which were subsequently screened using SECM for the ORR.[52] Of the combinations studies, coelectrodeposited Au-Pt catalysts showed the lowest onset potential. In another recent study, Schuhmann et al. employed SMCM to screen an extensive library of thin (0–5 nm) platinum films supported on mixed Ti/Nb oxide (6–27 at.% Nb) films to study support effects on the electrochemical activity.[53]It was found that

for Pt films with a nominal thickness of > 1 nm, the composition of the support material plays no significant role in the catalytic activity in the ORR. Below this threshold, catalytic activity depends strongly on the composition of the support.

Apart from employing SMCM to produce or screen catalytic spots, it is also commonly used to isolate single microscopic surface features on a heterogeneous surface. For example, local measurements have been performed on various spots on a (ZYA grade) HOPG surface, consisting of μm-sized graphite basal planes intersected by steps of one (or a few) atoms high,[48] with a spatial resolution better than the typical step spacing , demonstrating that the HOPG basal plane itself, and not just the step sites, supports high electron transfer activity. Similarly, droplet techniques can be used to probe "single-crystal" facets on polycrystalline or polyoriented substrates: Schultze et al. employed a droplet method (50–100 μm capillaries) to study the oxidation of single Zr and Ta grains[54] and the orientation dependent passivation and dissolution of Fe[55] on polycrystalline samples. Yan et al. employed a 400 μm capillary for studying single facets in a single-crystalline Au bead.[56]While these studies are not directly related to energy applications, they demonstrate the feasibility to conduct electrochemical measurements on single facets on a polycrystalline materials. In principle, such studies could be extended to perform pseudo-single crystal studies on energy-related electrocatalytic reactions without the need for expensive and difficult to handle single-crystal electrodes, although no such studies have yet been reported.

Although a strong point of SMCM is its ability to confine the working electrode to a small wetted area, it is very challenging to use it as an imaging technique.[47] Scanning electrochemical cell microscopy (SECCM, Figure 4c)[57,58] is a recent advance that addresses this issue. SECCM advances on SMCM by employing a dual-barrel theta pipet filled with electrolyte solution and a contact electrode serving as combined reference and counter electrodes (quasi-reference counter electrode;QRCE) in each channel. Similar to SMCM, the liquid meniscus at the end of the pipet is brought into contact with the substrate, and the investigated area is formed by the wetted area, which in turn is largely determined

by the diameter of the capillary. A small potential bias between the two QRCEs gives rise to a pipet conductance current, and by oscillating the pipet slightly in the *z*-direction (perpendicular to the substrate), an alternating conductance current component develops due to the periodic deformation of the contact meniscus. This alternating current component of the conductance current is strongly dependent on the meniscus height, and can be used as a feedback parameter to scan the droplet rapidly across the surface, thereby mapping surface topography and reactivity, a capability which is impossible to achieve with SMCM. The lateral resolution is determined by the capillary diameter (initially ~1 μm, currently < 400 nm).[57-59] In addition to the imaging capabilities, the potential bias between the QRCEs leads to the migration of charged species across the liquid meniscus, thereby enabling enhanced mass transport of charged species to and from the working electrode, allowing the study of very fast electrochemical reactions.[58]

SECCM has been employed to study the reactivity of platinum NPs on a CNT toward the ORR (Figure 4d).[59] SECCM was used to locate and record the potential-dependent reactivity of single particles, which were fully characterized by AFM and SEM. This experimental design allowed for direct correlation between the reactivity of a single particle with its physical characteristics and morphology. It was found that on a single particle level, ostensibly similar particles showed very different reactivities resulting from subtle variations in morphology on the nanoscale. Furthermore, it was shown that SECCM is sufficiently sensitive to measure very low currents (fA level), with the detection of only ~2500 electron transfer events in a spot during imaging.

Finally, research into the intrinsic electron transfer properties of a number of carbon materials that are employed as catalyst supports, such as HOPG,[60] CNTs,[61] graphene,[62] and boron-doped diamond,[63] is currently ongoing using SECCM to fully comprehend the subtle interplay between catalyst and support and its role in steering the catalytic activity and thereby allowing a rational choice of support material for catalytic systems in energy applications.

Conclusions and final remarks

In summary, we have presented a selective overview on the use of *in situ* scanning electrochemical probe microscopy (SEPM) techniques, such as scanning electrochemical microscopy, scanning micropipette contact method and scanning electrochemical cell microscopy, to study processes and materials related to energy applications and demonstrated the information that can be obtained with SEPM techniques. With a large drive toward the development of new *in situ* SEPM methods with nanoscale spatial resolution, we envisage SEPM will greatly contribute to energy research by unraveling nanoscale electrochemical processes and aid in obtaining fundamental insights needed for the development in new energy technologies.

Acknowledgments

We gratefully acknowledge financial support from a Marie Curie Intra European Fellowship within FP7 (project 275450 "VISELCAT") for SCSL and a European Research Council Advanced Investigator Grant (ERC-2009-AdG 247143 "QUANTIF") for PRU.

References

1. G.M. Whitesides, G.W. Crabtree, *Science* **315**, 796 (2007).

2. A.J. Bard, F.R.F. Fan, J. Kwak, O. Lev, *Anal. Chem.* **61**, 132 (1989).

3. J. Kwak, A.J. Bard, *Anal. Chem.* **61**, 1794 (1989).

4. S. Amemiya, A.J. Bard, F.R.F. Fan, M.V. Mirkin, P.R. Unwin, *Annu. Rev. Anal. Chem.* **1**, 95 (2008).

5. G. Wittstock, M. Burchardt, S.E. Pust, Y. Shen, C. Zhao, *Angew. Chem. Int. Ed.* **46**, 1584 (2007).

6. P. Sun, F.O. Laforge, M.V. Mirkin, *Phys. Chem. Chem. Phys.* **9**, 802 (2007).

7. M.V. Mirkin, W. Nogala, J. Velmurugan, Y. Wang, *Phys. Chem. Chem. Phys.* **13**, 21196 (2011).

8. S.M. Fonseca, A.L. Barker, S. Ahmed, T.J. Kemp, P.R. Unwin, *Chem. Commun.* (2003).

9. K. Eckhard, X. Chen, F. Turcu, W. Schuhmann, *Phys. Chem. Chem. Phys.* **8** (2006).

10. C. Batchelor-McAuley, E.J.F. Dickinson, N.V. Rees, K.E. Toghill, R.G. Compton, *Anal. Chem.* **84**, 669 (2011).

11. P. Bertoncello, *Energy Environ. Sci.* **3**, 1620 (2010).

12. S. Jayaraman, A.C. Hillier, *J. Phys. Chem. B* **107**, 5221 (2003).

13. S. Jayaraman, A.C. Hillier, *J. Comb. Chem.* **6**, 27 (2003).

14. M. Black, J. Cooper, P. McGinn, *Meas. Sci. Technol.* **16**, 174 (2005).

15. G. Lu, J.S. Cooper, P.J. McGinn, *J. Power Sources* **161**, 106 (2006).

16. J.L. Fernández, D.A. Walsh, A.J. Bard, *J. Am. Chem. Soc.* **127**, 357 (2004).

17. J.L. Fernández, V. Raghuveer, A. Manthiram, A.J. Bard, *J. Am. Chem. Soc.* **127**, 13100 (2005).

18. C.L. Lin, C.M. Sanchez-Sanchez, A.J. Bard, *Electrochem. Solid-State Lett.* **11**, B136 (2008).

19. D.A. Walsh, J.L. Fernandez, A.J. Bard, *J. Electrochem. Soc.* **153**, E99 (2006).

20. C.M. Sanchez-Sanchez, J. Solla-Gullon, F.J. Vidal-Iglesias, A. Aldaz, V. Montiel, E. Herrero, *J. Am. Chem. Soc.* **132**, 5622 (2010).

21. C.M. Sanchez-Sanchez, F.J. Vidal-Iglesias, J. Solla-Gullon, V. Montiel, A. Aldaz, J.M. Feliu, E. Herrero, *Electrochim. Acta* **55**, 8252 (2010).

22. J. Lee, H. Ye, S. Pan, A.J. Bard, *Anal. Chem.* **80**, 7445 (2008).

23. H. Ye, J. Lee, J.S. Jang, A.J. Bard, *J. Phys. Chem. C* **114**, 13322 (2010).

24. F. Zhang, V. Roznyatovskiy, F.-R.F. Fan, V. Lynch, J.L. Sessler, A.J. Bard, *J. Phys. Chem. C* **115**, 2592 (2011).

25. S.K. Haram, A.J. Bard, *J. Phys. Chem. B* **105**, 8192 (2001).

26. Y. Shen, K. Nonomura, D. Schlettwein, C. Zhao, G. Wittstock, *Chem. Eur. J.* **12**, 5832 (2006).

27. Y. Shen, U.M. Tefashe, K. Nonomura, T. Loewenstein, D. Schlettwein, G. Wittstock, *Electrochim. Acta* **55**, 458 (2009).

28. P. Sun, M.V. Mirkin, *Anal. Chem.* **78**, 6526 (2008).

29. Y. Shao, M.V. Mirkin, G. Fish, S. Kokotov, D. Palanker, A. Lewis, *Anal. Chem.* **69**, 1627 (1997).

30. H.L. Bonazza, J.L. Fernández, *J. Electroanal. Chem.* **650**, 75 (2010).

31. M. Shen, N. Arroyo-Currás, A.J. Bard, *Anal. Chem.* **83**, 9082 (2011).

32. J.V. Macpherson, C. Demaille, in *Scanning Electrochemical Microscopy, Second Edition,* A.J. Bard, M.V. Mirkin, Eds. (CRC Press, FL, 2012).

33. J.V. Macpherson, P.R. Unwin, *Anal. Chem.* **72**, 276 (2000).

34. C.E. Gardner, J.V. Macpherson, *Anal. Chem.* **74**, 576A (2002).

35. C. Kranz, J. Wiedemair, *Anal. Bioanal. Chem.* **390**, 239 (2008).

36. A. Davoodi, J. Pan, C. Leygraf, S. Norgren, *Electrochem. Solid St. Lett.*- **144**, B21 (2005).

37. Y. Zhu, D.E. Williams, *J. Electrochem. Soc.* **144**, L43 (1997).

38. A.R. Kucernak, P.B. Chowdhury, C.P. Wilde, G.H. Kelsall, Y.Y. Zhu, D.E. Williams, *Electrochim. Acta* **45**, 4483 (2000).

39. J. Meier, K.A. Friedrich, U. Stimming, *Faraday Discuss.* **121**, 365 (2002).

40. T.H. Treutler, G. Wittstock, *Electrochim. Acta* **48**, 2923 (2003).

41. E. Ammann, C. Beuret, P.F. Indermuhle, R. Kotz, N.F. de Rooij, H. Siegenthaler, *Electrochim. Acta* **47**, 327 (2001).

42. M. Ludwig, C. Kranz, W. Schuhmann, H.E. Gaub, *Rev. Sci. Instrum.* **66**, 2857 (1995).

43. A. Hengstenberg, C. Kranz, W. Schuhmann, *Chem. Eur. J.* **6**, 1547 (2000).

44. K. McKelvey, M.A. Edwards, P.R. Unwin, *Anal. Chem.* **82**, 6334 (2010).

45. P.L.T.M. Frederix, P.D. Bosshart, T. Akiyama, M. Chami, M.R. Gullo, J.J. Blackstock, K. Dooleweerdt, N.F. de Rooij, U. Staufer, A. Engel, *Nanotechnology* **19** (2008).

46. A. Anne, E. Cambril, A. Chovin, C. Demaille, C. Goyer, *ACS Nano* **3**, 2927 (2009).

47. M.M. Lohrengel, A. Moehring, M. Pilaski, *Electrochim. Acta* **47**, 137 (2001).

48. C.G. Williams, M.A. Edwards, A.L. Colley, J.V. Macpherson, P.R. Unwin, *Anal. Chem.* **81**, 2486 (2009).

49. T. Suter, H. Böhni, *Electrochim. Acta* **42**, 3275 (1997).

50. T.M. Day, P.R. Unwin, J.V. Macpherson, *Nano Lett.* **7**, 51 (2007).

51. P.V.Dudin, P.R. Unwin, J.V. Macpherson, *J. Phys. Chem. C*- **114**, 13241 (2010).

52. X. Chen, K. Eckhard, M. Zhou, M. Bron, W. Schuhmann, *Anal. Chem.* **81**, 7597 (2009).

53. D. Schaefer, C.C. Mardare, A. Savan, M.D. Sanchez, B. Mei, W. Xia, M. Muhler, A. Ludwig, W. Schuhmann, *Anal. Chem.* **83**, 1916 (2011).

54. J.W. Schultze, M. Pilaski, M.M. Lohrengel, U. Konig, *Faraday Discuss.* **121**, 211 (2002).

55. A. Schreiber, J.W. Schultze, M.M. Lohrengel, F. Karman, E. Kalman, *Electrochim. Acta*- **51**, 2625 (2006).56. J.W. Yan , C.F. Sun, X.S. Zhou, Y.A. Tang, B.W. Mao, *Electrochem. Commun.*- **9**, 2716 (2007).

57. N. Ebejer, M. Schnippering, A.W. Colburn, M.A. Edwards, P.R. Unwin, *Anal. Chem.* **82**, 9141 (2010).

58. M.E. Snowden, A.G. Guell, S.C.S. Lai, K. McKelvey, N. Ebejer, M.A. O'Connell, A.W. Colburn, P.R. Unwin, *Anal. Chem.* **84** (5), 2483 (2012).

59. S.C.S. Lai, P.V. Dudin, J.V. Macpherson, P.R. Unwin, *J. Am. Chem. Soc.* **133**, 10744 (2011).

60. S.C.S. Lai, A.N. Patel, K. McKelvey, P.R. Unwin, *Angew. Chem., Int. Ed.*- doi:10.1002/201200564 (2012)

61. A.G. Güell, N. Ebejer, M.E. Snowden, K. McKelvey, J.V. Macpherson, P.R. Unwin, *Proc. Nat. Acad. Sci.*- Accepted. (2012)

62. A.G. Güell, N.Ebejer, M.E. Snowden, J.V. Macpherson, P.R. Unwin, *J. Am. Chem. Soc.* **134**, 7258 (2012).

63. H.V. Patten, S.C.S. Lai, J.V. Macpherson, P.R. Unwin, *Anal. Chem.* - Accepted. (2012)

Figure Captions

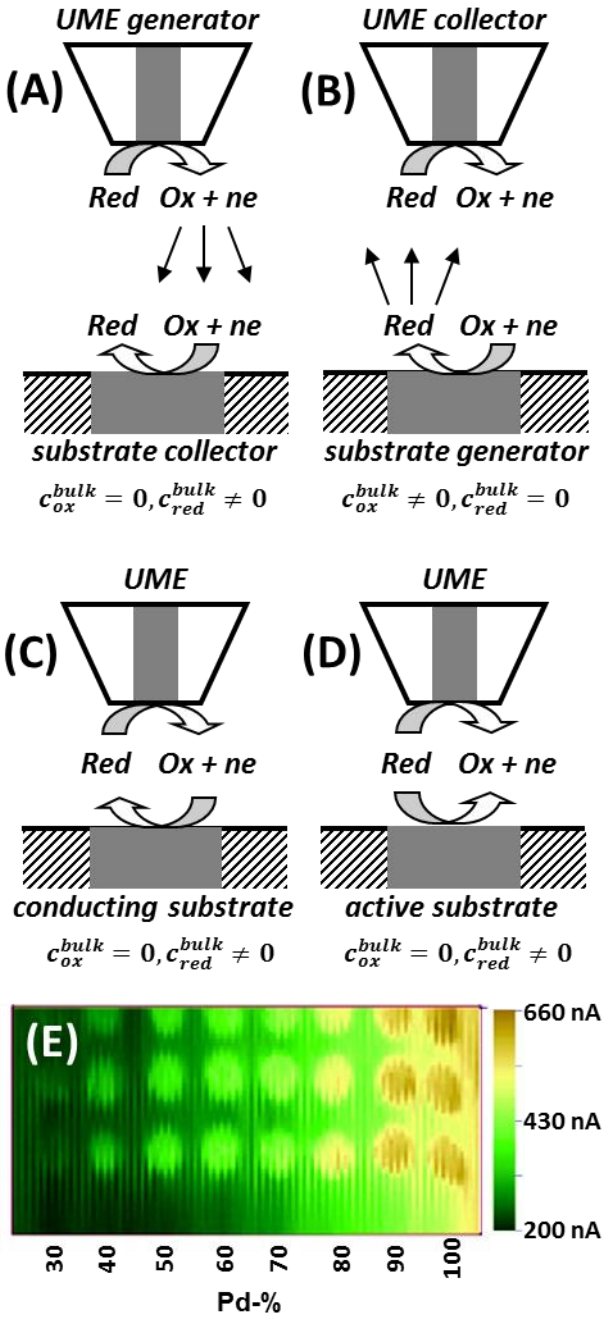

Figure 1. Scanning electrochemical microscopy (SECM). (a–d) Various modes of operation of SECM. The gray region in the tip indicates the electrode, while the white region corresponds to the insulating material. The gray region of the substrate corresponds to the electroactive region. (a) Tip generation/substrate collection (TG/SC) mode: the reactant for the substrate reaction is generated at the tip. The substrate current is followed as a measure of substrate reactivity. (b)

Substrate generation/tip collection (SG/TC) mode: the product for the substrate reaction is collected at the tip. The tip current is followed as a measure of substrate reactivity. (c) Feedback mode: the reactant of the tip reaction is regenerated by the substrate reaction. The (increase in) tip current is followed as a measure of substrate reactivity. (d) Shielding mode: The same reaction occurs at the tip and the substrate. A more active substrate leads to a decreased tip current. (UME: ultramicroelectrode, Red: reduced species, Ox: oxidized species, n: number of electrons, e: electron, $c^{bulk}{}_{ox}$: bulk concentration of the oxidized species, $c^{bulk}{}_{red}$: bulk concentration of the reduced species). (e) TG/SC image of oxygen reduction activity of binary Pd-Co alloys at 0.4 V versus. RHE (reversible hydrogen electrode) in 0.5 M H_2SO_4. The image shows the activity of an array of Pd-Co alloys with varying Pd content (three spots for each composition). Oxygen is produced electrochemically at the UME, as it is scanned over the substrate. The current passing through the substrate is recorded simultaneously as a function of UME position, so that a higher current is measured when the UME is positioned over a more active catalyst spot. Adapted with permission from Reference 16.

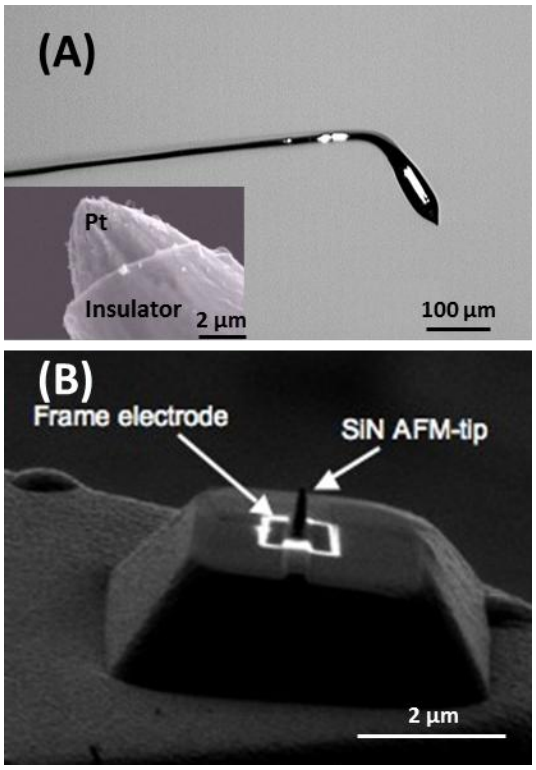

Figure 2. Combined scanning electrochemical microscopy – atomic force microscopy (SECM-AFM) probes. (a) Scanning electron micrograph of a SECM-AFM tip produced from a platinum wire. The platinum wire is etched to form a sharp tip and bent and flattened to form a force-sensing cantilever. The wire is covered in an insulating film except for the apex, leaving a micron-scale cone shaped electrode (inset) for SECM functionality. Adapted with permission from Reference 33. ©2000, American Chemical Society. (b) SECM-AFM tip with the SECM electrode set at a constant distance from the AFM tip. A conventional silicon nitride AFM probe is coated with a thin layer of gold and silicon nitride. The end of the tip is shaped with a focused ion beam, redefining the AFM tip and exposing a square shaped submicron gold electrode for SECM measurements. Image courtesy of Dr Christine Kranz.

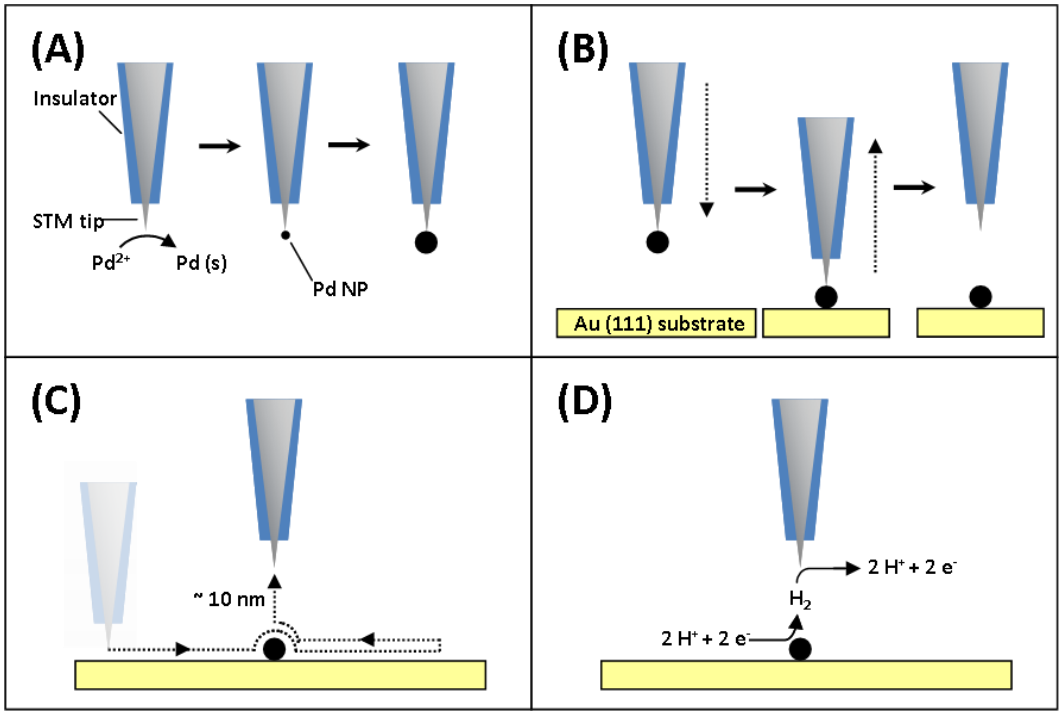

Figure 3. Schematic representation of the scanning electrochemical microscope – scanning tunneling microscope (SECM-STM) experiment performed by Stimming et al.[39] (a) A palladium nanoparticle (Pd NP) is formed at the end of a STM tip by electrodeposition. (b)The Pd NP is transferred to a gold (111) substrate. (c) The substrate is scanned by STM to locate and characterize the particle. Afterwards, the tip is positioned over the Pd NP and retracted *ca*. 10 nm. (d) The substrate is held at a potential at which protons are reduced to molecular hydrogen at the Pd NP, while the tip is held at a potential to oxidize the hydrogen produced in a SG/TC SECM experiment. Finally, steps (c-d) are repeated to obtain multiple measurements from the same Pd NP.

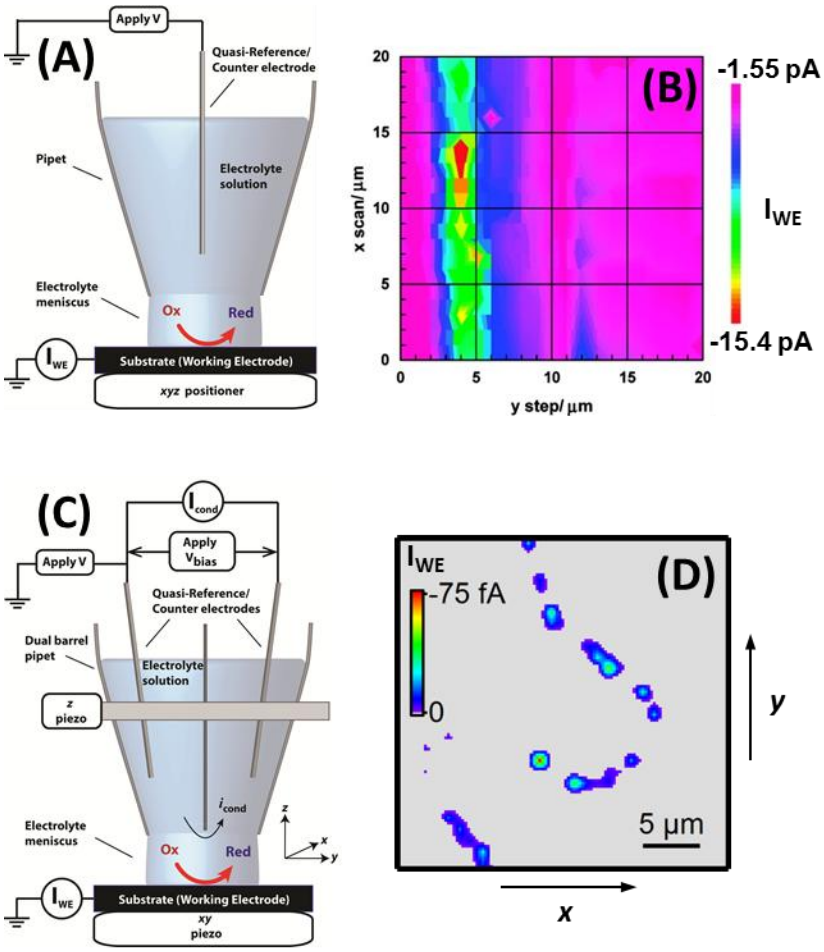

Figure 4. Capillary scanning electrochemical probe techniques. (a) Schematic setup for scanning micropipet contact method (SMCM). (I_{WE}: working electrode current) (b) SMCM image for the reduction of $Fe(CN)_6^{3-}$ on part of an 95%-5% Al-Cu alloy. The imaged area consists of Al with a Cu inclusion running from the bottom to the top of the image. The oxide protected aluminum shows very little current for the reduction of $Fe(CN)_6^{3-}$ (~ - 1.5 pA), with a significant enhancement of current on the copper inclusion, indicating that the electroactivity of this material is mostly localized at the copper inclusions. Adapted with permission from Reference 47. ©2010, American Chemical Society. (c) Schematic setup for scanning electrochemical cell microscopy (SECCM). (V_{bias}: potential bias between the two quasi-reference counter electrodes, I_{WE}: working electrode current, I_{cond}: conductance current) (d) SECCM image of ORR activity at individual Pt nanoparticles at 0.55 V versus RHE in 0.1 M H_2SO_4. A single walled carbon nanotube was decorated with platinum nanoparticles (Pt NPs) and investigated for ORR activity. The image shows that only the Pt NPs show appreciable ORR currents (up to 75 fA at this potential), and individual NPs can be clearly resolved, allowing structure-activity relationships for individual NPs to be established. Adapted with permission from Reference 56. ©2010, American Chemical Society.